Pure Appl. Chem., Vol. 72, No. 11, pp. 2149–2157, 2000.

Localization and bandwidth of the 3d-orbitals in magnetic Ni and Co clusters*

J. Morenzin, H. Kietzmann, P. S. Bechthold†, G. Ganteför‡, and W. Eberhardt

Institut für Festkörperforschung, Forschungszentrum Jülich, 52425 Jülich, Germany

Abstract: Photoelectron spectra of negatively charged Ni_n^-, Cu_n^-, and Co_n^- clusters are presented. The spectra of the Ni_n^- clusters contain information about the degree of localization of the 3d valence orbitals, which is strongly related to the magnetic properties. In the clusters with less than 7 atoms, the 3d orbitals seem to be almost totally localized. For Co_{13}^- we find indications of a narrowing of the 3d-derived valence "bandwidth" corresponding to a presumed high symmetry and a high degree of degeneracy of the 3d electronic states.

INTRODUCTION

Magnetism results from a preference of a high-spin ground state as a result of the tendency of the electrons to minimize their electrostatic repulsion (Hund's rule). Two electrons will form a triplet ground state if there are two almost degenerate single-particle orbitals available (corresponding to a small "bandwidth") and if the two electrons interact strongly (corresponding to a high degree of localization). Accordingly, atoms (zero bandwidth and total localization) are usually "magnetic" (i.e., they prefer a high spin ground state), while most bulk materials are nonmagnetic. Only very few bulk materials still exhibit magnetic properties. In all these cases, at least part of the valence electrons (in the case of Fe, Co, and Ni the 3d electrons) are still localized to some extend and the density of states at the Fermi energy is large, which corresponds to a small spacing between available single particle orbitals.

According to the above considerations, the magnetic moment per atom, which is basically a measure of the "magnetism", is found to decrease with increasing cluster size [1–3]. For the clusters with more than $n \approx 20$ atoms the magnetic moment per atom decreases from the maximum spin of the 3d-orbitals (1, 2, and 3 μ_{Bohr}/atom for Ni, Co, and Fe, respectively) to the bulk values (0.62, 1.74, and 2.21 μ_{Bohr}/atom for Ni, Co, and Fe, respectively [1]). The maximum values correspond to the approximate configurations of the atoms in the bulk ($\approx d^9s$, $\approx d^8s$, and $\approx d^7s$ for Ni, Co, and Fe, respectively).

The magnetic moments of the smallest Ni clusters with $n > 4$ show a behavior (Fig. 1), which deviates from the simple picture given above. The moments of the clusters with sizes $n = 5$–8 are considerably larger than the maximum spin of a Ni atom assuming a d^9s configuration (=1μ_{Bohr}/atom). For $n > 9$ the moments level at a value of 1.3 μ_{Bohr}/atom and decrease much slower with further increasing cluster size, approaching the bulk value at $n \approx 300$ [1]. The moment of Ni_{13} is smaller than the ones of the neighboring clusters.

To understand these results of Stern–Gerlach experiments, additional structural data are necessary [4]. In contrast to clusters of simple metals (e.g., Na, Ag) not many experimental data are available about the structure of Ni clusters. For the Ni dimer, experimental [5,6] and theoretical [7–12] publications agree that the atoms assume an almost pure d^9s configuration with the two Ni d^9 "cores" almost

*Lecture presented at the 10th International Conference on High Temperature Materials Chemistry (HTMC-X), Jülich, Germany, 10–14 April 2000. Other presentations are published in this issue, pp. 2101–2186.

†Corresponding author

‡Present address: Fakultät für Physik, Universität Konstanz, 78457 Konstanz

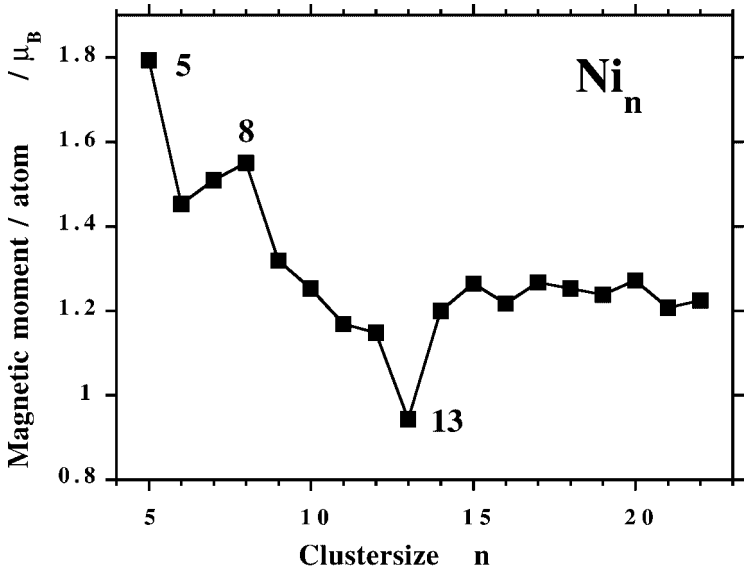

Fig. 1 Magnetic moments per atom in small Ni clusters detected in a Stern–Gerlach experiment (from Apsel *et al.* [3]).

noninteracting. The Ni-dimer bond is largely dominated by the interaction of the s- orbitals and is, therefore, very similar to the Cu dimer [5] with two noninteracting d^{10} cores.

To shed more light on the reasons for the special magnetic properties of the very small Ni clusters we study Ni and Co clusters using photoelectron spectroscopy of negatively charged particles. As we will show, the spectra contain information about the degree of 3d localization and the 3d valence bandwidth, which are both closely related to the magnetic properties.

EXPERIMENTAL

The experimental arrangement comprises three essential parts in a vacuum environment [13,14]. They are framed in the scheme of Fig. 2. The first part contains a laser-vaporization cluster source [15]. An intense focused laser pulse is used to vaporize a small amount of metal from a target rod, which performs a periodic spiral motion. This rod adjoins a tube, into which a pulse of inert helium gas is injected synchronously. Clusters grow inside this tube. The helium supports the condensation and cooling of the clusters by multiple collisions and serves simultaneously as a transport medium. The energy of condensation is partly transferred to the tube wall. At the end of the tube the cluster-helium mixture expands adiabatically into the vacuum vessel, thus further cooling the clusters and forming a supersonic molecular beam. The cooling occurs because part of the irregular thermal motion is transformed to center-of-mass motion. Note that in the adiabatic expansion the clusters do not reach thermal equilibrium. Translational, rotational, and vibrational temperatures are then defined by the population of the respective degrees of freedom.

The cluster beam always contains a mixture of clusters of various sizes. Mainly it is made up of neutrals but comprises also smaller amounts of charged clusters. They have to be selected and mass separated before information on clusters of a particular size can be obtained. Consequently, the beam is skimmed and enters the second part of the experiment, which consists of a time-of-flight mass spectrometer.

Since we are interested in cluster anions the negatively charged clusters are accelerated in a pulsed electric field of a Wiley–McLaren ion source [16]. Thereafter they enter a grounded drift tube and, depending on their times-of-flight, separate into a chain of bunches of defined cluster size.

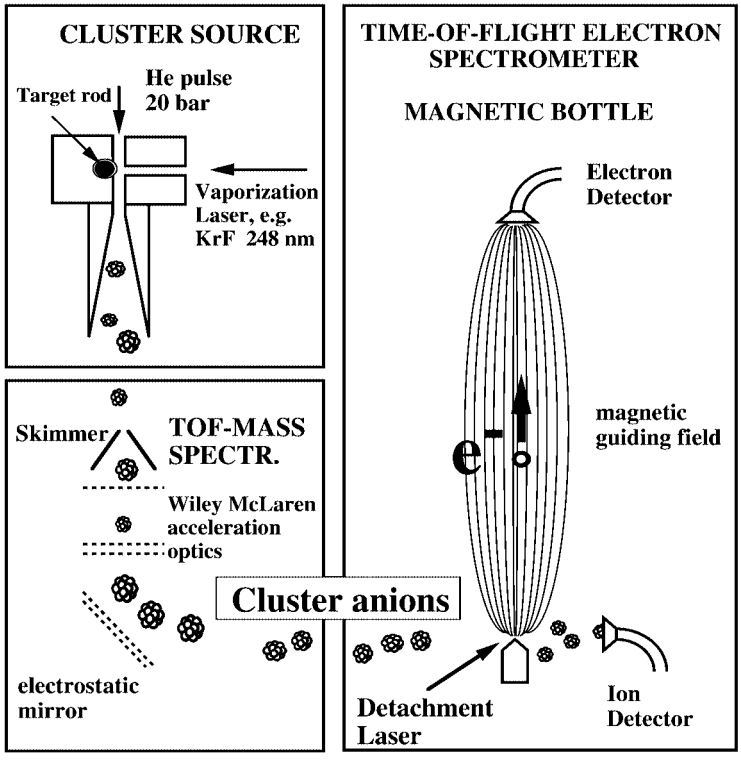

Fig. 2 Scheme of the three essential parts of the experiment. Cluster anions are formed in a laser vaporization cluster source and transferred to a pulsed time-of-flight mass spectrometer. The separated anions enter the source region of a "magnetic bottle"-type electron spectrometer where photoelectrons are detached. The kinetic energy of the photoelectrons is measured by a time-of-flight technique.

The drift tube contains an electrostatic mirror, which is used to deflect the cluster anions from the neutral beam path. An ion detector at the end of the drift region can be used to analyze their mass distribution. Since smaller clusters acquire larger velocities they arrive first. The others appear as the sequence of their masses.

Before the anions reach the ion detector they pass the source region of a "magnetic bottle" time-of-flight electron spectrometer, which is the third essential part of the experiment [13,14,17]. Here, a selected bunch of cluster anions is irradiated by a UV laser pulse (photon energy $h\nu = 4.0$ eV), and the kinetic energy of the detached electrons is measured. The advantage of the magnetic-bottle type spectrometer is that it permits the collection of all the emitted electrons irrespective of their direction of emission. A strongly inhomogeneous magnetic field at the location of the electron emission acts as a magnetic mirror and deflects all the electrons toward the electron detector. This sufficiently increases the electron yield. Prior to electron detachment a mass gate allows the selection of a particular cluster size. Clusters of other sizes are deflected out of the beam. Moreover, the cluster anions are decelerated prior to the electron detachment to prevent a Doppler shift of the emitted photoelectrons. Otherwise, the resolution of the spectrometer will be reduced. The spectrometer is calibrated with some atomic lines.

Ideally, the cluster anions are in their ground electronic state when they enter the electron spectrometer. This is, in fact, often the case. However, with transition-metal clusters, which usually exhibit a high density of states very close to their electronic ground state, some low lying excited states may also be populated. This will lead to the simultaneous presence of different isomers in the cluster beam.

The photoemission results in neutral final states, which are examined in the experiment. In the simple single-particle picture the binding energy (BE) of the electron in the anion is deduced from the difference of the photon energy hν and the measured electron kinetic energy E_{kin}:

$$BE = h\nu - E_{kin}.$$

The spectra then show the final electronic single particle states of the neutral cluster in the geometry of the anion. Thus, in this simple picture, the spectra are a direct mapping of the neutral clusters density of state, however with the geometry of the anion. Often, the geometrical structure of the anion does not deviate very much from the ground-state geometry of the neutral. In such a case, the peak at the lowest binding energy (i.e., the vertical detachment energy) corresponds to the ground state of the neutral cluster. However, its position may be shifted according to the Franck–Condon overlap of the anionic and the neutral cluster. In reality, the spectra are complicated by many body effects: multiplet splitting, shake up processes, and configuration-interaction effects may lead to considerable deviations from the simple picture [18–21].

The spectra of the Ni_n^- and Co_n^- clusters are very sensitive on the source conditions. Only if the cluster anions are effectively cooled in the seeding gas pronounced structures are observable. At less effective cooling conditions the spectra do not show sharp features. The cooling may be improved by integration of a waiting room into the condensation tube. From vibrationally resolved photoelectron spectra of various dimers we estimate the vibrational temperature of the clusters to be 250–350 K.

DATA AND DISCUSSION

Figure 2 displays a comparison of the photoelectron spectra of Ni_2^- and Cu_2^-. The spectra are in good agreement with earlier measurements [3,8–10]. For Ni_2 the signal to noise ratio is poor, which is due to the low relative intensity of the dimer in the mass spectrum. In both spectra a small peak A appears at low binding energy (BE ≈ 1 eV) and a larger feature B is visible at higher BE (Ni: ≈3.2 eV; Cu: ≈2.9 eV). For Cu, these two features are assigned to direct photoemission from the bonding σ (A) and antibonding σ* (B) 4s-derived orbitals [9,11]. The ground-state configuration of Cu_2^- is $(3d^{10})^2\sigma^2\sigma^*$, the ones of the two final states are $(3d^{10})^2\sigma^2$ (A) and $(3d^{10})^2\sigma\sigma^*$ (B), respectively.

The similarity of the main features A and B for Cu_2^- and Ni_2^- is surprising, because the bulk metals have different properties. The Cu atoms have filled $3d^{10}$ orbitals, while Ni is an open d-shell metal, the atom having a $3d^94s^1$ (^{3}D) ground state [22].

Following the analysis from Ho *et al.* [5] based on vibrationally resolved photoelectron spectra of the features A in both anion spectra, the similarity can be explained by the high degree of localization of the $3d^9$ orbitals in Ni. Both dimers are bound by the interaction of the 4s-orbitals forming a bonding 4s σ orbital. The 3d orbitals do not contribute significantly to the bond, because the "size" of the 3d-orbitals is much smaller than the one of the 4s orbitals. At the equilibrium distance of the dimers the overlap of the 3d orbitals is small. Although the $3d^9$ cores of the Ni atoms in the Ni dimer are not completely filled, they behave similar to highly localized "inner-shell" orbitals. Because of the difference of the radii of the 4s and 3d orbitals, s/d hybridization is weak in both dimers, too.

The differences in the two spectra (Fig. 3) are mostly due to the difference in the BEs of the 3d-derived features [23]. The 3d density of states in bulk Cu dominates at BEs larger than 2 eV with respect to the Fermi energy, while in Ni the 3d band is located just at the Fermi energy. This difference in BE of the 3d-derived features is also observable in the dimer spectra. In the spectrum of Cu_2 the broad feature at high BE (≈3.5 eV) is assigned to part of the 3d emission, while in the spectrum of Ni_2 the emission between 1.8–2.5 eV BE is assigned to the 3d orbitals. Even though the s/d hybridization is weak, it depends on the relative binding energies of the respective orbitals. Thus, the difference in binding energy of the features B in the spectra of Cu_2^- and Ni_2^- can be readily accounted for. According to the above considerations, the similarity of the 4s derived features in the spectra of Ni_2^- and Cu_2^- indicates a highly localized character of the Ni $3d^9$ cores similar to the closed shell $3d^{10}$ orbitals of the Cu atoms

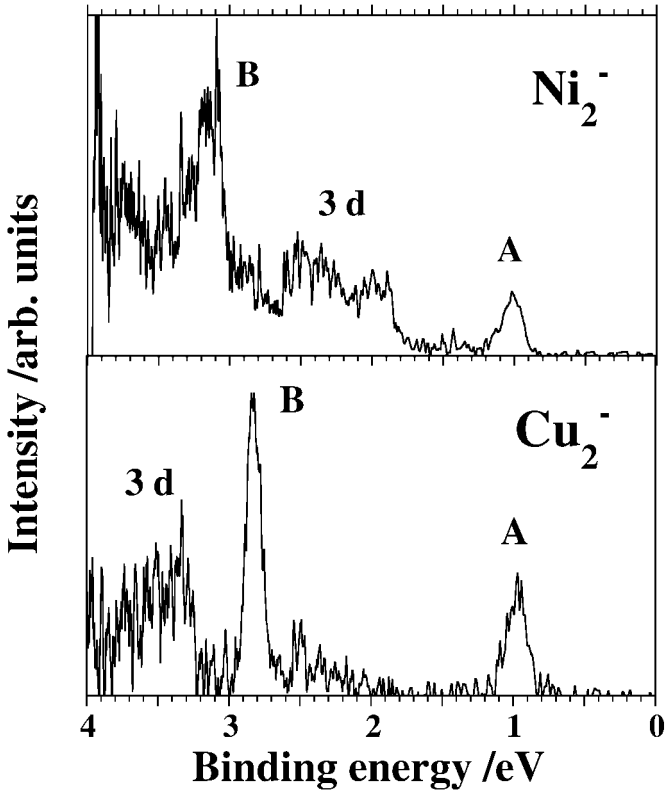

Fig. 3 Comparison of photoelectron spectra of Ni_2^- and Cu_2^-. The photon energy is hν = 4.0 eV. For a discussion of the marked features see text.

in the small Cu clusters. The two $3d^9$ cores in the Ni dimer can be viewed as "magnets" with a magnetic moment corresponding to the single vacancy (=l μ_{Bohr}/atom). Assuming vanishing s/d hybridization and spin-orbit interaction the two $3d^9$ cores can freely adjust to an external magnetic field, which is the fundamental property of superparamagnets [24].

Now we focus on the question up to which cluster size this similarity between the Cu and Ni cluster spectra might extend. With increasing cluster size the s/d hybridization is expected to increase and the 3d valence electrons should become more and more delocalized. The increasing coordination number of the metal d-atoms with increasing cluster size causes a d-band broadening, thus, supporting the delocalization process [25]. Similar effects occur on surfaces where larger magnetic moments have been predicted for the lower coordinated surface atoms with respect to the bulk [26]. In addition, such delocalization must be anticipated because of the itinerant character of the magnetism in bulk Ni. On the other hand, the decreasing shorter bond length with decreasing cluster size favors the participation of the d electrons in the bonding and, therefore, a delocalization of the d electrons with decreasing cluster size [10,11]. Therefore, a delicate balance is expected between exchange and correlation, between magnetism and chemical bonding, and between populating d and s orbitals. Our spectra indicate that the delocalization with increasing cluster size is more pronounced, even at the small cluster sizes considered here.

Figure 4 displays a comparison of the spectra of the even numbered Ni and Cu cluster anions for n = 4,6,8. We focus on the even numbered clusters, because the spectra of these Cu clusters display a characteristic peak at low BE. Such peaks are clearly visible in all Cu spectra [6,19,20] and, at almost the same BEs, in the spectra of Ni_4^- and Ni_6^-. For Ni_4^- there is even a feature at higher BE (B), which

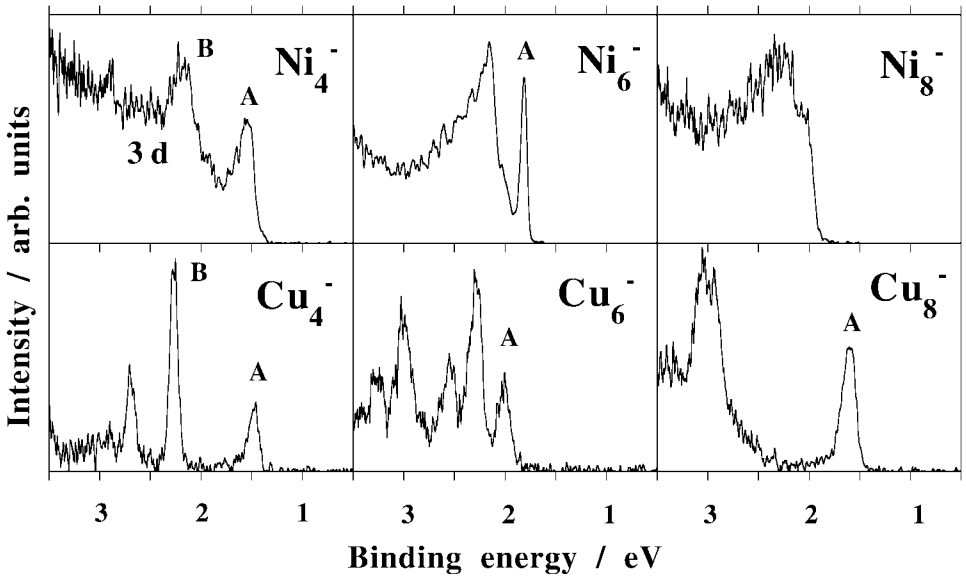

Fig. 4 Comparison of photoelectron spectra of Ni_4^-, Ni_6^-, and Ni_8^- with the corresponding data on Cu clusters. The photon energy is hν = 4.0 eV. For a discussion of the marked features see text.

resembles the corresponding peak in the spectrum of Cu_4^-. In contrast, the spectrum of Ni_8^- does not exhibit such a feature. We find that the spectra of the Ni_n^- clusters with n = 8–15 (not shown) display no pronounced features and are similar to the one of Ni_8^-. We conclude that the similarity between the spectra of the Ni_n^- and the Cu_n^- clusters vanishes at $n \approx 8$ indicating a collaps of the almost perfect localization of the Ni 3d orbitals. This observation is in agreement with the finding of a strong decrease of the magnetic moments per atom in small Ni clusters at $n \approx 8$ (Fig. 1).

However, the large values of the magnetic moments of the small Ni clusters cannot be explained within this framework. The maximum spin contribution of each Ni atom in a d^9s configuration is $1\mu_{Bohr}$. From energetic considerations it seems unlikely that more than one or two Ni atoms in these small clusters assume a d^8s^2 configuration (corresponding to $2\ \mu_{Bohr}$).

For itinerant (delocalized) electrons the orbital moment is not a good quantum number. Accordingly, the orbital momentum contribution to the magnetic moment in bulk Fe, Co, and Ni is quite small. For localized (core) electrons, such as the 4f electrons of the rare earths, however, the situation is different. In this case the orbital momentum is well defined and contributes significantly to the overall magnetic moment.

In order to explain the large magnetic moments observed for small Ni clusters, we propose an additional contribution from the orbital momentum of the electrons. Probably, in small Ni clusters the total magnetic moment is a superimposition of spin and orbital magnetic moments similar to free atoms (Hund's rules). The orbital contribution to the magnetic moment is much more sensitive to the degree of delocalization than the spin component. With increasing cluster size the orbital contribution is quenched already at very small cluster sizes, while the spin contribution decreases on a much larger size scale. At $n \approx 8$, there is a transition from highly localized 4f-like magnetism to 3d-like "pure spin" magnetism in agreement with our photoelectron data, which indicate an almost total localization of the 3d electrons in the smallest Ni clusters.

According to the results of the Stern–Gerlach experiment [3] displayed in Fig. 1 the magnetic moment per atom in Ni_{13} is considerably smaller than in all other clusters of that size range. The photoelectron spectrum of Ni_{13}^- is similar to the one of Ni_8^- and gives no indication of a special electronic structure of this cluster. However, we conducted a similar experiment on Co_n^- clusters.

The photoelectron spectra displayed in Fig. 5 show a multitude of peaks close to the emission threshold. For the larger clusters with $n > 10$ we assign these features to emission from occupied 3d-derived valence orbitals. These features will gradually develop into the 3d-emission peak of bulk Co located close to the Fermi energy. At higher BE the spectra show a smooth emission signal with a lower intensity, which we assign to emission from the 4s-derived valence orbitals dominating the density of states at higher BE in bulk Co. The range of BEs dominated by features tentatively assigned to 3d-emission has a minimum width for Co_{13}^-. A similar behavior has been observed for 3p-derived orbitals of small Al_n^- clusters [27]. A pronounced minimum of the "3p-bandwidth" has been found and related to the predicted high symmetry of this cluster. According to calculations, Al_{13}^- has most likely an icosahedral structure [28,29] and the low bandwidth might be caused by a high degree of degeneracy. Analoguously, the narrow 3d-bandwidth found for Co_{13}^- might also indicate a high symmetry and a correspondingly high degree of degeneracy. The spectra of the Co_n^- clusters (Fig. 5) have been obtained using a waiting room for most effective cooling. The spectra exhibit more fine structure than the earlier measurements from Yoshida *et al.* [30] indicating the importance of temperature for such kind of measurements. The spectra of the Ni_n^- clusters (e.g., Fig. 4) have been obtained using a less advanced source design, which might be the reason that we could not find a narrowing of the 3d-bandwidth for Ni_{13}^- yet. If we assume there is a similar narrowing of the 3d-bandwidth for the Ni_{13}^- cluster, this will be correlated with the local minimum of the magnetic moments for n = 13 (Fig. l). However, a small bandwidth indicating a higher density of states corresponds to a higher magnetic moment per atom (Stoner's law) in contradiction to Fig. 1. To solve this discrepancy, we propose again a separation into spin and angular magnetic moments. It might be possible, that in a symmetric, almost spherical, particle the orbital momenta of the 3d-electrons cancel each other resulting in a minimum contribution. Only the spin component contributes with its maximum value of 1 μ_{Bohr}/atom. However, this is just a tentative proposal, which needs further theoretical evaluation.

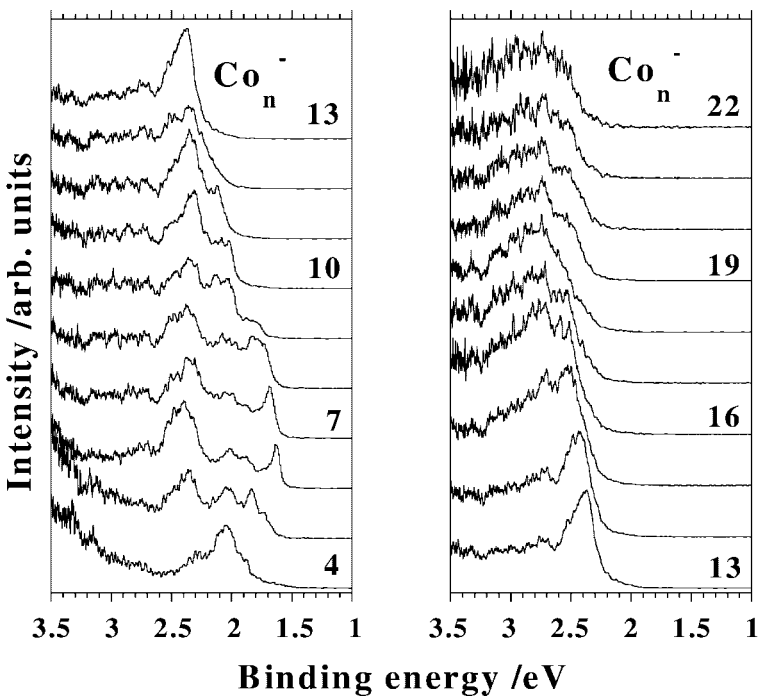

Fig. 5 Photoelectron spectra of Co_n^- clusters recorded using an improved cluster source design to generate more effectively cooled cluster anions. The photon energy is hν = 4.0 eV.

CONCLUSION

From a comparison of the 4s-derived features in the photoelectron spectra of Ni_n^- and Cu_n^- clusters we find indications for an almost total localization of the Ni 3d orbitals. This total localization vanishes at $n \approx 8$ and is accompanied by a steep decrease of the magnetic moments detected in a Stern–Gerlach experiment. These experimental observations can be explained by a transition from a 4f-like magnetism of the smallest Ni clusters to a "normal" 3d-like magnetism for the larger clusters (n > 8). In a rare-earth magnet the total magnetic moment consists of a spin and an orbital momentum component similar to free atoms. This explains the relatively high values of the magnetic moments per atom found for the smallest Ni clusters. The angular momentum component is very sensitive to electron delocalization and decreases rapidly with cluster size down to almost zero for bulk Ni.

The photoelectron spectra of Co_n^- clusters show a narrowing of the 3d- bandwidth for $n = 13$. This can be explained by a high symmetry of this cluster and a correspondingly higher degree of degeneracy of the valence orbitals analogous to the case of Al_{13}^-. Although we did not measure the corresponding Ni data yet, we expect to find a similar minimum of the 3d-bandwidth for Ni_n^- clusters. According to the Stoner rule an increased magnetic monent per atom of this cluster would be expected due to the higher density of states. However, for Ni_{13} a minimum of the magnetic moment has been detected. A tentative explanation for this behavior is given by a quenching of the orbital angular momentum due to the high symmetry of this cluster.

REFERENCES AND NOTES

1. I. M. L. Billas, A. Chatelain, W. A. de Heer. *Science* **265**, 1682 (1994).
2. I. M. L. Billas, A. Châtelain, W. A. de Heer, *J. Magn. Magn. Mater.* **168**, 64 (1997).
3. S. E. Apsel, J. W. Emmert, J. Deng, L. A. Bloomfield. *Phys. Rev. Lett.* **76**, 1441 (1996).
4. Experimentally, such information can only indirectly be obtained, e.g., from measurements of the chemical reactivity [a,b] and, particularly, spectroscopy [c]. [a] E. K. Parks, B. H. Weiller, P. S. Bechthold, W. F. Hoffmann, G. C. Niemann, L. G. Pobo, S. J. Riley. *J. Chem. Phys.* **88**, 1622 (1988); [b] E. K. Parks, L. Zhu, J. Ho, S. J. Riley. *J. Chem. Phys.* **100**, 7206 (1994); Ibid. **102**, 7377 (1995); [c] this work.
5. J. Ho, M. L. Polak, K. M. Ervin, W. C. Lineberger. *J. Chem. Phys.* **99**, 8542 (1993).
6. G. Ganteför and W. Eberhardt. *Phys. Rev. Lett.* **76**, 4975 (1996).
7. J. O. Noell, M. D. Newton, P. J. Hay, R. L. Martin, F. W. Bobrowicz. *J. Chem. Phys.* **73**, 2360 (1980).
8. I. Shim and K. A. Gingerich. In *The Physics and Chemistry of Small Clusters*, P. Jena, B. K. Rao, S. N. Khanna (Eds.), p. 523, Plenum Press, New York (1987).
9. S. E. Weber and P. Jena. *Chem. Phys. Lett.* **281**, 401 (1997).
10. M. Castro, C. Jamorski, D. R. Salahub. *Chem. Phys. Lett.* **271**, 133 (1997).
11. G. A. Cisneros, M. Castro, D. R. Salahub. *Int. J. Quantum Chem.* **75**, 847 (1999).
12. M. C. Michelini, R. Pis Diez, A. H. Jubert. *Int. J. Quantum Chem.* **70**, 693 (1998).
13. Chia-Yen Cha, G. Ganteför, W. Eberhardt. *Rev. Sci. Instrum.* **63**, 5661 (1992).
14. H. Handschuh, G. Ganteför, W. Eberhardt. *Rev. Sci. Instrum.* **66**, 3838 (1995).
15. D. E. Powers, S. G. Hansen, M. E. Geusic, A. C. Pulu, J. B. Hopkins, T. G. Dietz, M. A. Duncan, P. R. R. Langridge–Smith, R. E. Smalley. *J. Phys. Chem.* **86**, 2556 (1982).
16. W. C. Wiley and I. H. McLaren. *Rev. Sci. Instr.* **26**, 1150 (1955).
17. P. Kruit and F. H. Read. *J. Phys.* **E16**, 313 (1983).
18. O. Cheshnovsky, K. J. Taylor, J. Conceicao, R. E. Smalley. *Phys. Rev. Lett.* **64**, 1785 (1990).
19. Chia-Yen Cha, G. Ganteför, W.Eberhardt. *J. Chem. Phys.* **99**, 6308 (1993).
20. H. Handschuh, Chia-Yen Cha, P. S. Bechthold, G. Ganteför, W. Eberhardt. *J. Chem. Phys.* **102**, 6406 (1995).

21. C. Massobrio, A. Pasquarello, R. Car. *Phys. Rev. Lett.* **75**, 2104 (1995).
22. When weighted averages over the J components are used: C. E. Moore. *Atomic Energy Levels*, National Bureau of Standards, Circ. 467, Washington, DC (1952).
23. Multiplet splitting and shake up processes are neglected in this simplified analysis.
24. S. N. Khanna and S. Linderoth. *Phys. Rev. Lett.* **67**, 742 (1991).
25. F. Aguilera-Granja, S. Bouarab, M. J. Lopez, A. Vega, J. M. Montejano-Carrizales, M. P. Iniguez, J. A. Alonso. *Phys. Rev.* **B 57**, 12469 (1998).
26. S. Blügel. *Phys. Rev. Lett.* **68**, 851 (1992).
27. G. Ganteför and W. Eberhardt. *Chem. Phys. Lett.* **217**, 600 (1994).
28. O. Dolgounitcheva, V. G. Zakrzewski, J. V. Ortiz. *J. Chem. Phys.* **111**, 10762 (1999).
29. R. O. Jones. Density functional calculations, unpublished.
30. H. Yoshida, A. Terasaki, K. Kobayashi, M. Tsukada, T. Kondow. *J. Chem. Phys.* **102**, 5960 (1995).